Unveiling the Molecular Networks Underlying Cellular Impairment in Saccharomyces cerevisiae: Investigating the Effects of Magnesium oxide Nanoparticles on Cell Wall Integrity and Endoplasmic Reticulum Stress Response

Shraddha Chauhan

  Pohang University of Science and Technology

Raghuvir Singh Tomar

  rst@iiserb.ac.in

  IISER Bhopal: Indian Institute of Science Education and Research Bhopal

Abstract

Magnesium oxide nanoparticles (MgO-NPs) are highly versatile and have been extensively utilized in diverse industrial and biomedical applications due to their exceptional physical and chemical properties. However, the potential harms to human health and the environment from their use continue to be of great trepidation. In this study, we delved deep into the intricate molecular mechanisms underlying the detrimental effects of MgO-NPs on the growth and viability of the model yeast Saccharomyces cerevisiae. Our findings demonstrate that as the concentration of MgO-NPs increases, it leads to a dose-dependent reduction in the growth and viability of the yeast cells. We further investigated the underlying mechanisms of MgO-NP toxicity and found that it causes damage to the cell membrane, which in turn triggers an endoplasmic reticulum (ER) stress response. The response to ER stress involves an increase in the expression of genes that play a role in protein folding, maintaining protein quality, and removing misfolded proteins via ER-associated degradation (ERAD). In response to treatment with MgO-NPs, we observed the activation of the cell wall integrity (CWI) pathway, it caused the activation of chitin production genes and an increase in the amount of chitin in the cells. These findings highlight the multifaceted detrimental nature of MgO-NPs, which involve the interplay of various molecular networks and signaling pathways.

1. Introduction

Nanotechnology is a rapidly growing field which deals with the design, synthesis, characterization, and manipulation of materials at the nanoscale (1-100 nm). The distinct physical, chemical, and biological features of nanomaterials make them attractive for various applications, including in medicine, electronics, cosmetics, energy, and food industries. Despite the numerous advantages of nanomaterials, their impending detrimental consequences on human health and the environment, have raised concerns over the years. Therefore, it is essential to investigate the toxicity of nanomaterials to understand their potential risks and develop appropriate safety measures.

Nanoparticles (NPs) have become ubiquitous in modern technology and are widely used in various industrial, commercial, drug delivery, and other biomedical applications including their use in bioimaging, biosensors, drug delivery, and as antioxidants, with potential benefits for disease detection, treatment, and prevention due to their unique physicochemical properties (Vance et al. 2015; Namdari et al. 2017; Li et al. 2021; Abd et al. 2019). These materials have unique properties that allow them to interact with biomolecules, including components of the purinergic signaling system, which is an important transmitter system that uses purine nucleotides and nucleosides as chemical messengers. The interactions between nanomaterials and purinergic signaling components are not fully understood, but they can directly affect purinergic receptors, alter gene expression, activate inflammatory processes, and induce cell death (Ficerman et al. 2022). Graphene materials have potential for antibacterial, antiviral and antifungal applications due to their ability to control both Gram-positive and Gram-negative bacteria through oxidative stress, mechanical damage, wrapping, and electron transfer mechanisms. These nanomaterials exhibit profound antibacterial properties (Seifi and Kamali 2021). Magnesium oxide nanoparticles (MgO-

NPs) are one of the most extensively used NPs due to their high biocompatibility, low toxicity, and antimicrobial properties (Ahamad et al. 2023; Zhu et al. 2020). They have been used in various biomedical applications, including drug delivery, wound healing, and cancer therapy (Di et al. 2012; Nandhini et al. 2023; Pugazhendhi et al. 2019). Nevertheless, mounting evidence suggests that MgO-NPs can also pose significant risks to human health and the environment (Saravanakumar and Wang 2019; Mahmoud et al. 2016). Several studies have reported that MgO-NPs induce cytotoxicity, genotoxicity, and oxidative stress in various living cells, including human cells, animal cells, and microbial cells (Alavi et al. 2022; Amina et al. 2020). *Saccharomyces cerevisiae*, commonly known as baker's yeast, is a widely used model organism in various fields of research due to its genetic tractability, rapid growth, and ease of handling (Babele et al. 2018; Hanson 2018). Yeast cells are known to be sensitive to various environmental stressors, including NPs (Bao et al. 2015; Azad et al. 2014; Gola et al. 2015; Babele et al. 2018). Many fundamental cellular processes and molecular pathways, including cell wall integrity, protein folding, lipid metabolism, and stress response, are conserved across different organisms, including yeast and humans. By investigating the effects of nanoparticles on these conserved processes in yeast, we can gain insights into potential mechanisms of toxicity that may also be relevant in human cells. Therefore, studying the effects of MgO-NPs on yeast cells can provide valuable insights into the mechanisms underlying their cytotoxicity and potential risks to human health and the environment. Several studies have investigated the effects of NPs on yeast cells and identified some mechanisms underlying their toxicity. For instance, a study on investigates the potential destructive effects of zinc oxide nanoparticles on human cardiomyocytes has been carried out by Li and co-workers (Li et al. 2020). They investigated the harmful impact of zinc oxide nanoparticles on human cardiomyocytes and determine the mechanism behind these adverse effects, utilizing hiPSC-CMs as an in vitro model. The study on nanodiamond toxicity on the white rot fungus *Phanerochaete chrysosporium* was carried out, where results suggest that nanodiamond cause low toxicity and no effect on biomass gain or culture medium pH, but inhibition of certain decomposition activities at high concentrations due to oxidative stress (Ma et al. 2020).

Another study has been carried out to investigated the toxicity of different sizes and surface coatings/charges of silver nanoparticles on a fungal model, *Saccharomyces cerevisiae* BY4741. The results showed that the toxicity of silver nanoparticles was dependent on size and charge, and the coating influenced the mechanism of toxicity (Kasemets et al. 2019). Cellular membranes, including the plasma membrane and cell wall, are the first targets of NPs upon cell entry, and damage to these structures can lead to cellular dysfunction and death (Palocci et al. 2017). The cell wall, which is constituted β-glucans, chitin, and mannoproteins, plays an important role in maintaining cell shape, protecting the cell from osmotic stress, and regulating cellular processes such as cell division and differentiation (Lesage and Bussey 2006; Aguilar-Uscanga and Francois 2003). Endoplasmic reticulum (ER) stress response, which is triggered by various stressors such as unfolded proteins, oxidative stress, and calcium imbalance, is an essential mechanism for maintaining ER homeostasis and cell survival (Cao and Kaufman 2014).

The precise mechanisms underlying the interplay between cell wall damage and ER stress response triggered by MgO-NPs in yeast cells remain largely unknown. Understanding these mechanisms can

provide valuable insights into the potential risks associated with MgO-NPs and help develop effective strategies to mitigate their harmful effects. The goal of this study was to clarify the intricate crosstalk between multidimensional molecular networks underlying the complex cellular impairment triggered by MgO-NPs in *S. cerevisiae*. Therefore, we aimed to investigate the impact of magnesium oxide nanoparticles (MgO-NPs) on *Saccharomyces cerevisiae*, specifically on cell wall integrity, ER stress response, and cellular functions. The study intended to understand the mechanisms by which MgO-NPs may cause cellular damage and affect yeast viability.

2. Materials and methods

2.1 Synthesis and Characterization of MgO-NPs

The synthesis of MgO-NPs was carried out by co-precipitation method, where magnesium sulphate ($MgSO_4$) has been used a precursor salt. 0.5M $MgSO_4$ in 100ml distilled water has been made. The solution was kept under stirring condition for 30 minutes, 0.5M sodium hydroxide (NaOH) has been used as a reducing agent. NaOH has been added to the solution drop by drop under constant stirring, the white precipitation due to the reduction of salt has been formed. Subsequently, the solution was filtered and washed with methanol twice. The pellet was dried in hot air oven at 100°C for 2 h (Hornak 2021). The powdered nanoparticles were then collected and stored in airtight tube at room temperature. The as synthesized nanoparticles were characterized through scanning electron microscopy for their morphology. The elemental mapping to confirm the composition and distribution of the nanoparticle was carried out by Energy Dispersive X-ray (EDX) analysis. To check the bioavailability of MgO-NPs in water, the aggregation and sedimentation have been studied by UV-Vis spectroscopy. The desired concentration of MgO-NPs has been prepared by mixing the nanoparticle in DI water and the UV-Vis spectra were recorded by nanodrop at 0h and 3h time points where, the nanoparticle was subjected under constant shaking in incubator shaker.

2.2 *Saccharomyces cerevisiae* Strains, Growth Conditions, and Media

Table S1 contains a list of the *Saccharomyces cerevisiae* strains utilized in this study. The strains were maintained in YPD (1% Yeast extract, 2% Mycological-peptone and 2% Dextrose) and transformed strain with Atg8 plasmid was maintained in synthetic dropout media. The exponentially growing phase of the cells were obtained by incubating them at 30°C till the OD600 reaches ~1.0.

2.3 MgO-NPs Treatment on Yeast Cells

Saccharomyces cerevisiae cells growing in log phase (OD600 = ~1.0) were harvested (4000 rpm, 2 minutes), and washed twice with DI water. The cells were then suspended in DI water with variable concentration of MgO-NPs (0, 2, 4, 6 and 8 mg/ml), set one with 0 concentration of nanoparticle was considered as control. The treatment exposure has been given for 3h at 30°C in an incubator shaker under constant shaking at 200 rpm. The toxic effect of MgO-NPs on yeast cells were analyzed by spot

test assay and colony forming units (CFU) test as described by Sousa and coworkers, with anticipated reformations (Sousa et al. 2018).

2.4 Measurement of Cell Viability and Reactive Oxygen Species

The effect of MgO-NPs on yeast cell has been explored by appraising the viability of cells. The exponentially growing cells were incubated in DI water without (control) and with MgO-NPs at 30°C for 3h in an incubator shaker at 180 rpm. The cells were then plated over YPD agar media and the number of colonies were counted to calculate the percent growth by dividing each group with the control group (without treatment). To reckon the yeast cell death, we performed propidium iodide (PI) staining method. After 3h of treatment with MgO-NPs, the cells were harvested and suspended in phosphate buffer saline (PBS) buffer (pH 7.5) with 20 µg/ml PI (prepared in PBS buffer) for 5 min. Under a fluorescent microscope (ZEISS ApoTome) equipped with an RFP filter set, the stained cells were viewed.

The measurement of intracellular reactive oxygen species (ROS) was measured by oxidant sensing fluorescent probe 2,7-Dichlorodihydrofluorescein diacetate (DCFH-DA). This is a dye that can permeate through cell membranes and is nonpolar. Inside the cell, it is modified by esterases to form a polar derivative called DCFH, which is not fluorescent. When intracellular ROS oxidize the DCFH, it is converted to a highly fluorescent form called 2,7-dichlorofluorescein (DCF). The detection of ROS was checked by keeping the wild type yeast cells under untreated and treated condition as described concentrations of NPs and then incubated with 10 µM DCFH-DA for 30 minutes. The cells were washed twice with chilled PBS and then observed under fluorescence microscope with GFP filter.

2.5 Cell Wall Staining, Measurement of Chitin and Lipid Droplets (LDs)

Cell wall is the primary layer through which any foreign particle interacts to enter the cell, therefore the first pathway that could be triggered is cell wall integrity (CWI) pathway. In the yeast the cell wall integrity pathway is activated when sensors on plasma membrane senses the stress and transmit the signal to Slt2 (Mpk1) MAP kinase. The activation of Slt2 indicates the instigation of CWI pathway (Gola et al. 2015; Babele et al. 2018). The cell tries to rescue itself from the stress by upregulating the chitin synthesis to make the cell wall more integrated, therefore to identify the cell wall stress we checked the expression of chitin under treated and untreated conditions.

The investigation of MgO-NPs on expression of cell wall synthesis genes such as *CHS1, CHS3*, and *CHS5*, cells were treated with variable concentration of nanoparticle in treated and untreated conditions for 3h and harvested for RNA extraction. The chitin measurement was done by imperiling the yeast cells for staining with 20 µg ml^{-1} Calcofluor White (CFW) for 5 minutes and then washed thrice with PBS. The cells were then visualized by fluorescence microscope with DAPI filter (excitation λ: 325 nm, emission λ: 435 nm).

To check the intracellular LDs content, yeast cells were harvested and washed twice with DI water and then resuspended in PBS buffer. The cells were then stained with 10 µg ml^{-1} Bodipy for 5 min. After staining the cells were washed twice with PBS buffer and then envisaged under fluorescence microscope with FITC (Bodipy; excitation λ: 488 nm, emission λ: 520 nm) filter set (Qiu and Simon 2016).

2.6 Instrumental Analysis

2.6.1 Fluorescence Microscopic

The effect of MgO-NPs on the yeast strains have been tested by inoculating single colony of wild type and transformed strains into 5ml YPD media and incubated at 30°C in an incubator shaker. Successive day the cells were inoculated to fresh YPD medium at 0.2 OD600nm and cultured till the exponential phase has been reached. The cells were then harvested and washed twice with DI water. The subsequent treatment with and without (control) MgO-NPs (4mg/ml) in DI water has been given for 3h in an incubator shaker at 200rpm. The treated and untreated cells were visualized under fluorescence microscope with appropriate excitation and emission range. The experiment was conducted using a 63x oil immersion objective lens on a ZEISS ApoTome.2 fluorescence microscope. The images were captured and then processed using the ZEN-2012 (Blue Edition) apotome software.

2.6.2 PCR and Western blotting analysis

To perform gene expression analysis, 1µg of DNA-free RNA was used to reverse transcribe into cDNA through iScript cDNA Synthesis Kit (Bio-Rad, India). The PCR reactions were carried out using respective primers. The transcription levels were compared against the expression level of actin (ACT). The data of expression level of PCR product was visualized by ImageQuant™ LAS 4000 mini (GE Healthcare Life Sciences).

To perform western blotting analysis, the wild type yeast cells (BY4743) were subjected to treatment and control with selected doses (0, 2, 4, 6, and 8 mg/ml) of MgO-NPs, for 3h at 24°C. The extraction of total protein was performed by previously described methods of our laboratory (Golla et al. 2016). The antibody phospho-Slt2 (p44/42) was used for analyzing CWI pathway. To check the epigenetics alteration caused by nanoparticle toxicity have been evaluated by checking histone modifications, where antibodies named H3K4me2 (Abcam, 8895), H3K4me3 (Abcam,32356), H3K56Ac (Sigma, SAB4200328), H3K23Ac (Abcam, 46982) and H3K9Ac (Abcam 69830) were used. Anti-Tbp was taken as a loading control. IRDye® 800CW Goat anti-Rabbit IgG (1:15000) was used as secondary antibody. Odyssey infrared-imager (LI-COR biosciences) was used to scan the blots for protein detection.

2.7 Statistical Validation

The experiments were performed in triplicate, and the reported values represent the average and standard deviation of three replicates. Significant differences between the treatments were determined using one-way ANOVA ($P < 0.05$). The statistical analysis was performed in MS office excel.

3. Results

3.1 Characterization of the Synthesized MgO Nanoparticles

The nanoparticles were synthesized through chemical reduction method and the characterization of the morphology has been done through SEM. The mechanism of the chemical reduction method involves the reduction of metal ions in a solution by a reducing agent to form nanoparticles. In this case, the magnesium ions were reduced by a reducing agent. The cylindrical shape of the nanoparticles is due to the specific reaction conditions, such as the concentration of reducing agent (0.5M), pH (12), temperature (60°C), and reaction time (30 min). The characterization of the nanoparticles using SEM suggests that they have a narrow size distribution with an average size of 64.95 nm (Fig S1 A, B). The elemental analysis using Energy Dispersive X-ray Spectroscopy (EDS) confirms the presence of Mg and O in the synthesized nanoparticles. The elemental analysis confirms the formation of purified nanoparticles containing 32.7% Mg and 67.2% O (Fig S1C). The sedimentation and aggregation analysis of MgO-NPs were performed in DI water at the incubation of 0h and 3h and then analyzed by UV-Vis spectroscopy (Thermo Scientifc, NanoDrop 8000) (Fig S1D). The peaks of nanoparticles at variable concentration were significant to each other that indicates that the nanoparticles were effusively disseminated throughout the incubation time without aggregation or sedimentation.

3.2 Concentration Dependent Toxicity of MgO-NPs on *Saccharomyces cerevisiae*

To identify the inhibitory effect of MgO-NPs on the growth of yeast (BY4743), the cells were treated with nanoparticles (0, 2, 4, 6, and 8 mg/ml) and spot test and CFU were carried out. The findings of the experiment suggest that the growth of yeast cells (BY4743) is inhibited by MgO-NPs in a dose-dependent manner. At lower concentrations of 2 mg/ml, the inhibitory effect was minimal, while at higher concentrations (6 and 8 mg/ml), the inhibition was more than 50%, indicating a radical diminution in the growth of yeast cells (6mg = ~ 33% and 8mg ~ 29% cell survival) (Fig. 1). To understand the mechanism of this inhibitory effect, we utilized propidium iodide (PI) staining to evaluate damage of cell membrane damage. The use of PI is predicated on the fact that it cannot penetrate live cells but can stain dead cells, thereby indicating the impact of MgO-NPs on damage of cell membrane. The fluorescence microscopy images showed a consistent increase in PI-positive dead cells at increasing concentrations of MgO-NPs, compared to the untreated control cells (Fig S2).

3.3 MgO-NPs Trigger the Accumulation of Intracellular ROS and Cause Cell Wall Perturbation

Chitin is a crucial component of the fungal cell wall, and its synthesis is tightly regulated by various genes. Under stress conditions, such as those induced by exposure to MgO-NPs, the fungal cell wall is subjected to perturbation and damage. To cope with this damage, the cell increases the synthesis of chitin, which acts as a reinforcing agent and helps in maintaining the structural integrity of the cell wall. The cell under stress condition increases the synthesis of chitin to rescue itself from cell wall damage.

Therefore, identifying the level of chitin could be the indictor of cell wall perturbation. Consequently, study here investigated the impact of magnesium oxide nanoparticles (MgO-NPs) on the cell wall perturbation and chitin synthesis in cells. We examined the chitin content in the control and treated cells and stained with CFW, the visualization after staining indicates that the untreated cells have uniformed chitin layer over the cell surface, whereas under stress condition (treatment with MgO-NPs) caused the increased level of chitin in the cell (Fig. 2a). The gene expression analysis demonstrates that under stress conditions induced by MgO-NPs, there is an upregulation of expression of chitin synthesis genes (*CHS1*, *CHS3*, and *CHS5*), resulting in increased chitin content in the cell (Fig. 2b, c). The upregulation of chitin synthesis genes, such as *CHS1, CHS3*, and *CHS5*, is likely responsible for the increased chitin content in the cell. These genes are known to play important roles in chitin synthesis and are essential for maintaining the structural integrity of the fungal cell wall. *CHS1* is involved in the synthesis of chitin microfibrils, which are essential for the integrity of the cell wall. *CHS3* is responsible for the synthesis of chitin at the septum, which is essential for cytokinesis, while *CHS5* is involved in the synthesis of chitin in the cell wall. These genes have been selected for their expression analysis as they are crucial for the synthesis of chitin and the maintenance of cell wall integrity. Few other reports on cell wall stress also indicates that the chitin level increases under stress conditions (Bulik et al. 2003; Ribeiro et al. 2021; Babele et al. 2018).

Further we also analyzed the ROS accumulation, in few cases the toxicity of nanoparticles in not ROS dependent but generally the cells have high ROS content under elevated stress ailments. It is known that ROS play a role in a number of biological activities, including cell signaling, apoptosis, and stress responses. The treated and untreated cells were stained with DCFH-DA and visualized under microscopy. In this study, the staining of cells with DCFH-DA revealed that the ROS accumulation is dose-dependent, with higher concentrations of MgO-NPs resulting in increased ROS production in the cells (Fig S3).

3.4 MgO-NPs Impaired the Function of Mitochondria, Alters Lipid Metabolism, Endoplasmic Reticulum, Cause Lipid Droplet Formation and Induce Autophagy

The effect of MgO-NPs on lipid metabolism have been examined by utilizing genomically tagged molecular markers of Fas1 (mcherry) and Fas2 (GFP). In the case of normal cells (untreated) the diffused cytosolic distribution of Fas1 and Fas2 protein was observed while they get accumulated and formed foci under treatment condition (MgO-NPs exposure) (Fig. 3a, b).

Protein folding is a crucial process that occurs within the ER of eukaryotic cells. Proteins that are misfolded or incorrectly folded can lead to cause a distress to the cell. Hsp104 is a protein that belongs to the Hsp100 family, which is involved in protein folding, disaggregation, and quality control in the cell. Hsp104 has been chosen to check ER protein folding because it has been shown to be involved in the disaggregation of misfolded proteins in yeast. In normal cells, the Hsp104-GFP protein is distributed homogeneously throughout the ER, indicating proper protein folding. However, in treated cells, the

Hsp104-GFP protein is distributed in a punctuated manner, suggesting that protein folding is impaired (Fig. 3c). As a result, punctuated distribution of Hsp104 in treated cells suggests impaired protein folding, highlighting the importance of Hsp104 and other ER chaperones in maintaining protein homeostasis in the cell.

The ER is a complex organelle responsible for many essential cellular functions, including protein synthesis, folding, and trafficking. The ER can be divided into two main regions: the nuclear envelope-associated ER and the peripheral ER, which is located near the plasma membrane. The structure and organization of the ER are critical for its proper function, and any disruption to the ER structure can have severe consequences for the cell. To examine the structure of the ER, we have used a transformed yeast strain with ss-dsRed-HDEL, which is a marker of the nuclear and cortical ER junction. The results showed that in untreated cells, the dsRed-HDEL marker was localized in the peripheral ER near the plasma membrane and the nuclear envelope, which is consistent with the known distribution of ER in yeast cells (Fig. 3e). However, in cells treated with MgO-NP, the dsRed-HDEL localization was disturbed, and perturbations in the ER periphery were observed. This suggests that MgO-NP treatment disrupts the organization of the ER, potentially leading to functional deficits.

To investigate the effect of MgO-NPs on mitochondrial structure and function, Psd1 was chosen because it is directly involved in the biosynthesis of phospholipids, which are critical components of mitochondrial membranes. The disruption of Psd1 activity indicates that the integrity of mitochondrial membranes is compromised, which could result in impaired mitochondrial function. When we used transformed strain tagged with Psd1 under treated and untreated conditions we observed disrupted structure in the fluorescence microscopy images, which suggests that MgO-NPs cause mitochondrial stress by inducing oxidative damage to mitochondrial membranes (Fig. 3d). This damage may lead to the disruption of Psd1 activity and ultimately, the impairment of mitochondrial function.

The ERMES complex is a critical structure that connects the ER and mitochondria. We used genomically tagged Mdm34-GFP to observe cellular organization of ER and mitochondria. The results indicated the distribution of Mdm34-GFP in untreated and treated cells. In untreated cells, the localization of Mdm34-GFP was uniform, indicating the presence of a stable ERMES complex. However, in treated cells, the distribution of Mdm34-GFP was scattered, suggesting an alteration in the ERMES complex (Fig. 3f).

To further confirm, we also examined the activation of unfolded protein response (UPR) pathway. ER is a repository of various nascent polypeptides, they are properly folded and provided structural and functional attributes. We analyzed the splicing of *HAC1* mRNA which act as an indicator of UPR activation due to ER stress.

We have analyzed the expression of *HAC1, PSD1, IRE 1, KAR2* (Fig. 4c) and other stress related genes (FigS4). It seems that high concentration is inhibiting the activation of UPR (Fig. 4). The induction in the expression of *IRE1* and *PSD1* gene while nanoparticle treatment also indicates the activation of UPR, that cause ER stress and mitochondrial disfunction (Fig. 4c). The results showed that untreated cells also show basal level of splicing and at higher concentration (6mg/ml) dose, the cells activate the UPR

pathway to rescue themselves from stress but increasing the dose more doesn't show any salvaging mechanism to overcome ER stress. With all these results it can be affirmed that MgO-NPs are affecting lipid homeostasis, alters mitochondrial function and cause ER stress.

Lipid droplets are intracellular compartments that are used for storing neutral lipid essential for stable metabolism of lipid and energy homeostasis (Yu et al. 2015). As we observed ER stress due to nanoparticle toxicity, we tried to determine whether it is inducing the LD formation and autophagy. The detection of LD formation was done by staining the untreated and treated cells with Bodipy, the untreated conditions few LDs were formed, while in case of treatment large number of LDs accumulation has been seen (Fig. 4a). The intensity of fluorescence has been increased with increased LDs formation at high stress condition. The possible mechanism by which nanoparticles are inducing LD accumulation could be cell wall damage. The previous data suggests that due to cell wall damage, ER stress and UPR response have been activated, also, ER stress is a known activator of LDs accumulation (Jacquier et al. 2011). Therefore, we suggest that accumulation of LDs is concomitant to the nanoparticles stress on cell wall. Other than that ROS accumulation could also be accompanying the LDs formation, as the MgO-NPs toxicity is also triggering ROS formation, consequently it may also play a role in LDs formation (Yilancioglu et al. 2014).

To evaluate the induction of autophagy due to nanotoxicity we used GFP-tagged Atg8 construct and transformed into the wild type cells of yeast. The Atg8 protein functions as cargo recognition and then recruited to autophagosomes (Lee and Lee 2016; Du et al. 2023). When transformed cells were subjected to MgO-NPs treatment and visualized under microscopy, we observed high fluorescence intensity that indicates the distribution of GFP-tagged Atg8 in the cell, while the less fluorescence intensity in the untreated cells indicate that only basal level of autophagy is proceeding in the cells (Fig. 4b). The increase in GFP-tagged Atg8 fluorescence intensity in treated yeast cells compared to untreated cells could indicate an upregulation of autophagy in response to MgO-NP treatment. In response to cellular stress, such as oxidative damage or ER stress caused by MgO-NP treatment, cells may upregulate autophagy to remove damaged or toxic components and promote cell survival. Atg8 is a protein that is involved in the formation of autophagosomes, which are double-membrane vesicles that engulf cellular components for degradation. When autophagy is induced, Atg8 is recruited to the autophagosomal membrane and becomes incorporated into the membrane structure. By tagging Atg8 with GFP, we can visualize the distribution of autophagosomes in cells and monitor changes in autophagy levels.

Therefore, the increase in GFP-tagged Atg8 fluorescence intensity in treated yeast cells compared to untreated cells suggests that MgO-NP treatment induces an upregulation of autophagy in response to cellular stress. The cells are attempting to remove damaged or toxic components to maintain cellular homeostasis and promote cell survival. We also checked the expression level of some genes responsible for apoptosis like *NUC1, YCA1* and *AIF1*. The results suggested that the cell death increases with increased dose of MgO-NPs (Fig S4 B).

We have also studied the expression of genes *BAG7, SRL3, OYE3, KDX1*, and *GRX5* in yeast stress is important because these genes are known to play crucial roles of yeast in the response to various environmental stress condition. The PCR results indicate the significant induction in few of the genes while increasing the MgO-NPs dose (2, 4mg/ml), while other shows reduction even at low level of dose. However, there is decline in the expression at higher concentrations (Fig. 5).

3.6 MgO Nanoparticles Cause Oxidative Stress and Activation of CWI Pathway

To clandestine the exertion of MgO-NPs toxicity on CWI signaling pathway, we examined the null mutants of CWI pathway. The treatment with nanoparticles on null mutants displayed significant reduction in growth of MAPK(Slt2), MEKs (Mkk1/2), Rlm1 and MEKK (Bck1) (Fig. 6a). While the effect on Gas1, Wsc1 and Bck1 null mutant growth was moderate (Fig. 6a, b). The experimental aftermaths that CWI pathway is important for cells to combat the toxicity of MgO-NPs. Further substantiation of CWI pathway instigation was carried out by checking the activation of CWI Slt2 (MAP kinase). The immunoblotting results indicates that with increasing the dose of nanoparticles, the phosphorylation level of Slt2 increases as compared to the level of untreated cells (Fig. 6c). As ROS accumulation is also causing the increased oxidative stress, we further examined the expression level of some oxidative stress responsive genes like *SOD1, GSH1, CTT1*. The superoxide dismutase removes the $O^{\bullet-}_2$ to provide the defense against oxidative damage, therefore we observed overexpression of *SOD1* under treatment conditions (Fig S4 A). Similarly, *CTT1* also protects the cell from hydrogen peroxide cause oxidative damage, but the expression level analysis of *CTT1* shows that the under certain level of dose i.e., 2 mg/ml the upregulation of the expression have been observed but increasing the dose from 4-6mg/ml the expression level falls (Fig S4 A). We have also checked the level of glutathione to validate the oxidative stress level on yeast and the expression level of *GSH1, GSH2* falls that indicates that MgO-NPs are causing oxidative stress to the cells (Fig S4 A).

3.7 MgO-NPs Effect on Epigenetic Marks

The epigenetics targets of MgO-NPs have been identified by treating wild type and histone mutant strains of yeast with variable concentration of nanoparticles (Fig. 7). The cell cytotoxicity assay performed on histone H3 and H4 mutants indicate that few selected strains (H3R69K, H3K122A, H3K122R and H4S47D) are sensitive to MgO nanoparticle. The results of the study showed that only certain strains of yeast with specific mutations in the histone genes were sensitive to MgO nanoparticles. This suggests that the presence of lysine, arginine, and serine residues in H3 and H4 histone proteins at particular positions are crucial for cell survival under MgO-NPs stress. These residues are known to be involved in the binding of histones to DNA and other proteins, and their alteration could affect the structure and function of chromatin, leading to cell death (Fig. 7c).

To further evaluate the effect of MgO-NPs on histones we analyzed the post translational modifications (PTMs) like H3K56Ac, H3K4me, H3K9Ac, H3K23Ac by immunoblotting. The study also revealed that MgO nanoparticles induce changes in the PTMs of histone proteins, particularly in the case of H3K4me, where

the high dose of nanoparticles enhanced the methylation level. H3K4me is a histone modification that is associated with active gene expression, and its alteration could affect the regulation of gene expression and other cellular processes (Fig S5).

4. Discussion

The present study investigated the effect of MgO-NPs on the growth and viability of yeast cells (BY4743). The results indicate that increasing the concentration of nanoparticles above 2 mg/ml leads to a significant reduction in the growth and viability of yeast cells. The reduction in cell survivability was dose-dependent, and at higher concentrations (6 and 8 mg/ml), it caused a radical diminution in the growth of yeast cells. These findings suggest that MgO-NPs have a potent inhibitory effect on the growth and viability of yeast cells. The results of both CFU and spot test assays were consistent, and they established a dose-dependent reduction in the growth and viability of yeast cells. To further investigate the mechanism of growth inhibition, we assessed the effect of MgO-NPs on cell membrane integrity by exposing the cells to propidium iodide (PI) staining. The images of fluorescence microscopy indicated that the increase in concentration of nanoparticle resulted in a constant increase in PI positive dead cells as compared to untreated cells. These findings suggest that MgO-NPs cause cell membrane damage in yeast cells, leading to cell death. Chitin is one of the major polysaccharide elements of yeast cell wall, that provides mechanical strength and stability and make the cell wall rigid for foreign particles (Babele et al. 2018). Therefore, we examined cell wall perturbation and the subsequent increase in chitin content in cells. The results indicated that MgO-NPs triggered the accumulation of intracellular ROS and caused cell wall perturbation, which in turn led to the upregulation of chitin synthesis genes and increased chitin content in cells. The visualization of chitin content using CFW staining confirmed that untreated cells have a uniform chitin layer over the cell surface, whereas stress conditions caused an increase in chitin content in cells. This observation was further corroborated by the upregulation of chitin synthesis genes (*CHS1, CHS3*, and *CHS5*) in response to MgO-NP treatment. These results provide evidence for the link between cell wall perturbation, chitin synthesis, and ROS accumulation in cells treated with MgO-NPs. These findings are correlates with the previous reports on stress tolerance mechanisms on yeast. (Ribeiro et al. 2021; Babele et al. 2018).

Fatty acid synthesis involves the action of enzymes such as fas1 and fas2 that elongate carbon chains to produce saturated palmitic and stearic acids. These fatty acids undergo further modification in the endoplasmic reticulum through the activity of the enzyme fatty acid desaturase, which converts them into monounsaturated fatty acids like palmitoleic and oleic acids. The results of the current study shows that MgO-NPs cause the accumulation of Fas1 and Fas2 protein, which are involved in fatty acid synthesis, and disrupt their normal cytosolic distribution. The presence of foci formed by fas1 and fas2 throughout the cytosol is a sign of disrupted lipid homeostasis. The creation of saturated fatty acids like palmitic acid and an increase in fatty acid synthase activity may be the root of this disruption. These processes may also result in an excess of reactive oxygen species and lipotoxicity, which may eventually result in cell wall destruction. The ER is crucial for cellular lipid production, redox homeostasis, and protein folding. The UPR is a signaling pathway within cells gets activated when there is an excess of misfolded

proteins. It plays a role in regulating lipid levels in eukaryotes. In addition to the UPR, a heat shock response (HSR) is triggered when misfolded or denatured proteins accumulate in the cytoplasm and do not enter the secretory pathway. This is known as the cytosolic UPR, as described by (Hou et al. in 2014). The accumulation and expression of heat shock proteins, such as Hsp104-GFP, is commonly used as a way to identify the presence of cytosolic misfolded protein aggregates.

MgO-NP treatment also leads to a perturbation in the peripheral ER and punctuated distribution of Hsp104 protein, indicating that the proper folding of proteins in ER is disrupted. Additionally, the structure of the mitochondria is disrupted, and the Psd1 enzyme involved in lipid biosynthesis is affected. The study further suggests that MgO-NPs may cause changes in the ERMES complex, which is responsible for the transfer of lipids, metabolites, and calcium ions between the ER and mitochondria. The altered distribution of Mdm34-GFP, a component of the ERMES complex, observed in treated cells suggests that the ERMES complex is indeed affected by MgO-NP treatment. These disruptions ultimately lead to cellular stress and activation of the UPR pathway. The UPR pathway is a cellular mechanism that responds to ER stress by inducing the expression of genes involved in protein folding, quality control, and degradation. The UPR pathway is regulated by inositol-requiring enzyme 1 (*IER1*), which is a transmembrane kinase and endonuclease. The study showed that the expression of *IRE1* and *PSD1* genes, involved in the UPR pathway, was induced upon MgO-NP treatment. This indicates that MgO-NPs are causing ER stress, which in turn activates the UPR pathway. The study also depicted that the splicing of HAC1 mRNA, which is an indicator of UPR activation, was increased upon MgO-NP treatment. However, the increase in splicing was only observed at a moderate concentration of MgO-NPs (6mg/ml), while higher concentrations did not show any salvaging mechanism to overcome ER stress. This suggests that MgO-NPs may have a biphasic effect on the UPR pathway, with low to moderate concentrations inducing UPR activation, while high concentrations inhibiting UPR activation.

The CWI signaling pathway is crucial in defending yeast cells against MgO-NP toxicity. The null mutants of the CWI pathway showed a significant reduction in growth, indicating that this pathway is essential for cell viability when nanoparticles are present. The effect of MgO-NPs on Gas1, Wsc1, and Bck1 null mutant growth was moderate, indicating that these genes may have a less significant role in the response to nanoparticles. Furthermore, the activation of the CWI Slt2 MAP kinase was found to increase with increasing doses of MgO-NPs, indicating that the CWI pathway is triggered by the presence of nanoparticles. This suggests that the pathway is involved in the cellular response to stress caused by nanoparticles. Additionally, the study examined the expression level of oxidative stress responsive genes like *SOD1, GSH1*, and *CTT1*. *SOD1* encodes for superoxide dismutase, an enzyme that helps to protect the cell from damage caused by ROS. Proteins, lipids, and DNA damage can be caused by ROS, which are byproducts of normal cellular metabolism. *SOD1* helps to neutralize these ROS by converting superoxide radicals into innocuous hydrogen peroxide. *CTT1* encodes for catalase, another enzyme that helps to protect the cell from ROS. Catalase breaks down hydrogen peroxide into water and oxygen, thus preventing the accumulation of harmful ROS. In the presence of oxidative stress, such as exposure to high levels of ROS, the expression of *SOD1* and *CTT1* is upregulated in yeast cells. This allows the cells to better cope with the increased oxidative stress by neutralizing ROS more efficiently.

The overexpression of *SOD1* was observed under treatment conditions, suggesting that the superoxide dismutase enzyme is involved in removing reactive oxygen species and protecting the cell from oxidative damage. The expression level of *CTT1* showed a biphasic response, with upregulation observed at a dose of 2mg/ml but a decrease in expression level at higher doses of MgO-NPs. Similarly, the expression level of *GSH1* and *GSH2* fell, indicating that MgO-NPs are causing oxidative stress to the cells. *GSH1* and *GSH2* are two important genes in yeast that encode enzymes involved in the synthesis of glutathione (GSH), a potent antioxidant that plays a critical role in protecting cells against oxidative stress.

Activation of the CWI pathway and overexpression of *SOD1* were observed in response to nanoparticle treatment, indicating that oxidative stress is involved in the cellular response to nanoparticles.

A noteworthy observation made during our studies was that the exposure to MgO-NPs resulted in an augmentation of cellular lipid droplets (LDs). LDs are essential for lipid metabolism and energy homeostasis, and their accumulation is associated with ER stress and UPR response. In this study, LD formation was observed in treated cells, indicating that nanoparticles induce ER stress and UPR response, leading to LD accumulation. Additionally, ROS accumulation could also contribute to LD formation, as nanoparticles toxicity is known to trigger ROS production. Autophagy is a natural process within cells that facilitates the breakdown and disposal of various cellular components such as damaged organelles and protein aggregates. The results presented in this study demonstrate that autophagy is induced in response to nanoparticle toxicity. The observed increase in GFP-tagged Atg8 distribution indicates an increase in autophagic activity in treated cells compared to untreated cells. The increased expression of genes responsible for apoptosis, including *NUC1, YCA1*, and *AIF1*, suggests that cell death increases with increased dose of MgO-NPs. *NUC1* is a gene that encodes a nuclease enzyme that is responsible for the degradation of nuclear DNA during apoptosis. The enzyme is activated during the late stages of apoptosis and breaks down the chromatin into small fragments. *YCA1*, also known as caspase-activated DNase, is a gene that encodes a DNase enzyme that is activated by caspases during apoptosis. The enzyme cleaves DNA into fragments, which are subsequently degraded by other nucleases, including *NUC1*. The activation of *YCA1* is an early event in the apoptotic pathway and is required for the fragmentation of chromatin and DNA. AIF1, or apoptosis-inducing factor 1, is a gene that encodes a mitochondrial protein that plays a critical role in apoptosis. *AIF1* is released from the mitochondria during apoptosis and translocate to the nucleus, where it induces chromatin condensation and DNA fragmentation. The presence of *AIF1* is a marker for the activation of the mitochondrial pathway of apoptosis. The induction of apoptosis may occur as a result of oxidative stress and damage to cellular components, leading to cell death. The influence of various environmental factors on gene expression is becoming more evident, as they are known to cause changes in covalent histone modifications. These modifications play a critical role in cell signaling, protein function, and genome maintenance. Our study aimed to assess the impact of MgO-NPs on the growth of histone mutants. Therefore, we also tested the epigenetic targets of MgO-NPs using wild type and histone mutant strains of yeast has revealed interesting findings. The results indicate that certain histone mutations in yeast cells make them more susceptible to MgO-NPs induced stress, suggesting the importance of specific amino acid residues in histone proteins in cell survival under nanoparticle stress. Specifically, the presence of lysine, arginine,

and serine at particular positions in H3 and H4 histone proteins seems to be crucial for cell survival under MgO-NPs stress. The analysis of post-translational modifications (PTMs) of histone proteins under MgO-NPs stress has also yielded interesting results. The high dose of MgO-NPs has been found to enhance the methylation level of H3K4me, which is a known marker for active gene expression. This suggests that MgO-NPs may affect gene expression by altering the histone methylation levels. The altered PTMs of histones observed in this study may also have implications for the regulation of other cellular processes that are mediated by chromatin structure, such as DNA replication, repair, and transcription.

5. Conclusion

The purpose of the study was to investigate the effect of MgO-NPs on the growth and viability of yeast cells, as well as to explore the mechanisms underlying any observed effects. The study aimed to determine whether increasing concentrations of MgO-NPs would lead to a reduction in yeast cell growth and viability and to identify any cellular processes that might be disrupted by MgO-NPs. The main findings of the study were that the reduction in growth and viability of yeast cells under MgO-NPs treatment are dose-dependent. The study also found that MgO-NPs caused cell membrane damage, leading to cell death. Additionally, the study showed that MgO-NPs triggered the accumulation of intracellular ROS, causing cell wall perturbation, which led to the upregulation of chitin synthesis genes and increased chitin content in cells. Finally, the study found that MgO-NPs disrupted lipid homeostasis, leading to the overproduction of reactive oxygen species and lipotoxicity, ultimately causing damage to the cell wall. Overall, the study provides insight into the potential mechanisms underlying the harmful effects of MgO-NPs on yeast cells.

Declarations

1. Abd Elkodous M, El-Sayyad GS, Abdelrahman IY, et al (2019) Therapeutic and diagnostic potential of nanomaterials for enhanced biomedical applications. Colloids Surf B Biointerfaces 180:411-428

2. Aguilar-Uscanga B, Francois JM (2003) A study of the yeast cell wall composition and structure in response to growth conditions and mode of cultivation. Lett. Appl. Microbiol 37:268-274.

3. Ahamad L, Khan AK, Khan M, Farid O, Alam M (2023) Exploring the nano-fungicidal efficacy of green synthesized magnesium oxide nanoparticles (MgO NPs) on the development, physiology, and infection of carrot (Daucus carota L.) with Alternaria leaf blight (ALB): Molecular docking. J. Integr. Agric, 1-20.

4. Alavi M, Rai M, Martinez F, Kahrizi D, Khan, H, Rose Alencar De Menezes I, et al (2022) The efficiency of metal, metal oxide, and metalloid nanoparticles against cancer cells and bacterial pathogens: different mechanisms of action. CMBR 2:10-21.

5. Amina M, Al Musayeib NM, Alarfaj NA, El-Tohamy MF, Oraby HF, Al Hamoud GA, et al (2020) Biogenic green synthesis of MgO nanoparticles using Saussurea costus biomasses for a comprehensive detection of their antimicrobial, cytotoxicity against MCF-7 breast cancer cells and photocatalysis potentials. PLoS One 15:e0237567.

6. Azad GK, Singh V, Mandal P, Singh P, Golla U, Baranwal S, et al (2014) Ebselen induces reactive oxygen species (ROS)-mediated cytotoxicity in Saccharomyces cerevisiae with inhibition of glutamate dehydrogenase being a target. FEBS open bio 4:77-89.

7. Babele PK, Thakre PK, Kumawat, R, Tomar, RS (2018) Zinc oxide nanoparticles induce toxicity by affecting cell wall integrity pathway, mitochondrial function and lipid homeostasis in Saccharomyces cerevisiae. Chemosphere 213:65-75.

8. Bao S, Lu Q, Fang T, Dai H, Zhang C (2015) Assessment of the toxicity of CuO nanoparticles by using Saccharomyces cerevisiae mutants with multiple genes deleted. AEM 81:8098-8107.

9. Bulik DA, Olczak M, Lucero HA, Osmond BC, Robbins PW, Specht CA (2003) Chitin synthesis in Saccharomyces cerevisiae in response to supplementation of growth medium with glucosamine and cell wall stress. Eukaryot Cell 2:886-900.

10. Cao SS, Kaufman RJ (2014) Endoplasmic reticulum stress and oxidative stress in cell fate decision and human disease. ARS 21:396-413.

11. Di DR, He ZZ, Sun ZQ, Liu J (2012) A new nano-cryosurgical modality for tumor treatment using biodegradable MgO nanoparticles. NBM 8:1233-1241.

12. Du J, Zhao H, Zhu M, Dong Y, Peng L, Li J, et al (2023) Atg8 and Ire1 in combination regulate the autophagy-related endoplasmic reticulum stress response in Candida albicans. Res. Microbiol 174:103996.

13. Ficerman W, Wiśniewski M, Roszek K (2022) Interactions of nanomaterials with cell signalling systems–focus on purines-mediated pathways. Colloids Surf. B Biointerfaces, 112919.

14. Golla U, Bandi G, Tomar RS (2015) Molecular cytotoxicity mechanisms of allyl alcohol (acrolein) in budding yeast. Chem. Res. Toxicol 28:1246-1264.

15. Hanson PK (2018) Saccharomyces cerevisiae: a unicellular model genetic organism of enduring importance. Curr. Protoc. Essent. Lab. Tech 16:e21.

16. Hornak, J (2021) Synthesis, properties, and selected technical applications of magnesium oxide nanoparticles: a review. Int. J. Mol. Sci 22:12752.

17. Hou J, Tang H, Liu Z, Österlund T, Nielsen J, Petranovic D (2014) Management of the endoplasmic reticulum stress by activation of the heat shock response in yeast. FEMS yeast Res 14:481-494.

18. Jacquier N, Choudhary V, Mari M, Toulmay A, Reggiori F, Schneiter R (2011) Lipid droplets are functionally connected to the endoplasmic reticulum in Saccharomyces cerevisiae. J. Cell Sci 124:2424-2437.

19. Kasemets K, Käosaar S, Vija H, Fascio U, Mantecca P (2019) Toxicity of differently sized and charged silver nanoparticles to yeast Saccharomyces cerevisiae BY4741: a nano-biointeraction perspective. Nanotoxicology 13:1041-1059.

20. Lee YK, Lee JA (2016) Role of the mammalian ATG8/LC3 family in autophagy: differential and compensatory roles in the spatiotemporal regulation of autophagy. BMB reports 49:424.

21. Lesage G, Bussey H (2006) Cell wall assembly in Saccharomyces cerevisiae. MMBR 70:317-343.

22. Li H, Yin D, Li W, Tang Q, Zou L, Peng Q (2021) Polydopamine-based nanomaterials and their potentials in advanced drug delivery and therapy. Colloids Surf. B Biointerfaces 199: 111502.

23. Li Y, Li F, Zhang L, Zhang C, Peng H, Lan F et al (2020) Zinc oxide nanoparticles induce mitochondrial biogenesis impairment and cardiac dysfunction in human iPSC-derived cardiomyocytes. Int. J. Nanomedicine 15:2669-2683.

24. Ma Q, Zhang Q, Yang S, Yilihamu A, Shi M, Ouyang B et al (2020) Toxicity of nanodiamonds to white rot fungi Phanerochaete chrysosporium through oxidative stress. Colloids Surf. B Biointerfaces 187:110658.

25. Mahmoud A, Ezgi Ö, Merve A, Özhan G (2016) In vitro toxicological assessment of magnesium oxide nanoparticle exposure in several mammalian cell types. Int. J. Toxicol 35: 429-437.

26. Namdari M, Eatemadi A, Soleimaninejad M, Hammed AT (2017) A brief review on the application of nanoparticle enclosed herbal medicine for the treatment of infective endocarditis. Biomed. Pharmacother 87:321-331.

27. Nandhini SN, Sisubalan N, Vijayan A, Karthikeyan C, Gnanaraj M, Gideon DAM, et al (2023) Recent advances in green synthesized nanoparticles for bactericidal and wound healing applications. Heliyon 9:e13128.

28. Palocci C, Valletta A, Chronopoulou L, Donati L, Bramosanti M, Brasili E (2017) Endocytic pathways involved in PLGA nanoparticle uptake by grapevine cells and role of cell wall and membrane in size selection. Plant Cell Rep 36:1917-1928.

29. Pugazhendhi A, Prabhu R, Muruganantham K, Shanmuganathan R, Natarajan S (2019) Anticancer, antimicrobial and photocatalytic activities of green synthesized magnesium oxide nanoparticles (MgO NPs) using aqueous extract of Sargassum wightii. J. Photochem. Photobiol. B, Biol. 190:86-97.

30. Qiu B, Simon MC (2016) BODIPY 493/503 staining of neutral lipid droplets for microscopy and quantification by flow cytometry. Bio-protocol 6:e1912-e1912.

31. Ribeiro RA, Vitorino MV, Godinho CP, Bourbon-Melo N, Robalo TT, Fernandes et al (2021) Yeast adaptive response to acetic acid stress involves structural alterations and increased stiffness of the cell wall. Sci. Rep, 11:12652.

32. Saravanakumar K, Wang MH (2019) Biogenic silver embedded magnesium oxide nanoparticles induce the cytotoxicity in human prostate cancer cells. Adv Powder Technol, 30:786-794.

33. Seifi T, Kamali AR (2021) Anti-pathogenic activity of graphene nanomaterials: A review. Colloids Surf. B Biointerfaces 199:111509.

34. Sousa CA, Soares HM, Soares EV (2018) Nickel oxide (NiO) nanoparticles disturb physiology and induce cell death in the yeast Saccharomyces cerevisiae. Appl. Microbiol. Biotechnol 102:2827-2838.

35. Vance ME, Kuiken T, Vejerano EP, McGinnis SP, Hochella Jr MF, Rejeski D, Hull MS (2015) Nanotechnology in the real world: Redeveloping the nanomaterial consumer products inventory. Beilstein J. Nanotechnol 6:1769-1780.

36. Yilancioglu K, Cokol M, Pastirmaci I, Erman B, Cetiner S (2014) Oxidative stress is a mediator for increased lipid accumulation in a newly isolated Dunaliella salina strain. PloS one 9:e91957.

37. Yu Q, Liu Z, Xu H, Zhang B, Zhang M, Li M (2015) TiO 2 nanoparticles promote the production of unsaturated fatty acids (UFAs) fighting against oxidative stress in Pichia pastoris. RSC Adv 5:41033-41040.

38. Zhu D, Chen Y, Yang H, Wang S, Wang X, Zhang S, Chen H (2020) Synthesis and characterization of magnesium oxide nanoparticle-containing biochar composites for efficient phosphorus removal from aqueous solution. Chemosphere 247:125847.

References

Figures

Figure 1

Cell cytotoxicity of MgO-NPs on *S. cerevisiae* (**a**) Spreading for CFU analysis of wild type 4743 cells under treated and untreated condition for 3h, (**b**) Spot test assay of similar treatment condition after 48h, (**c**) Cell survival graph of CFU, (**d**) Graph of percent PI-positive cells in control and MgO-NPs treated conditions. * indicates a significant difference between the untreated and treated groups (P<0.05).
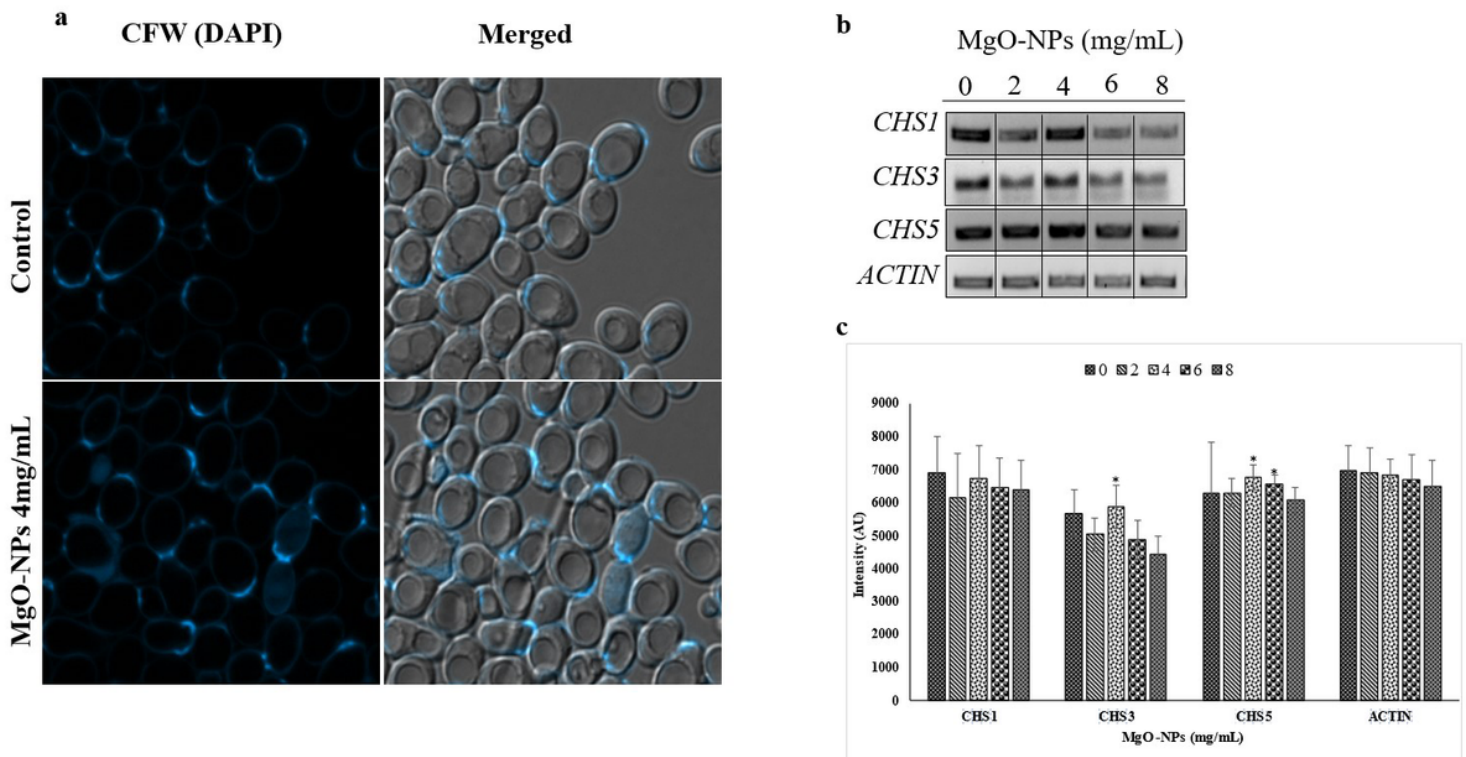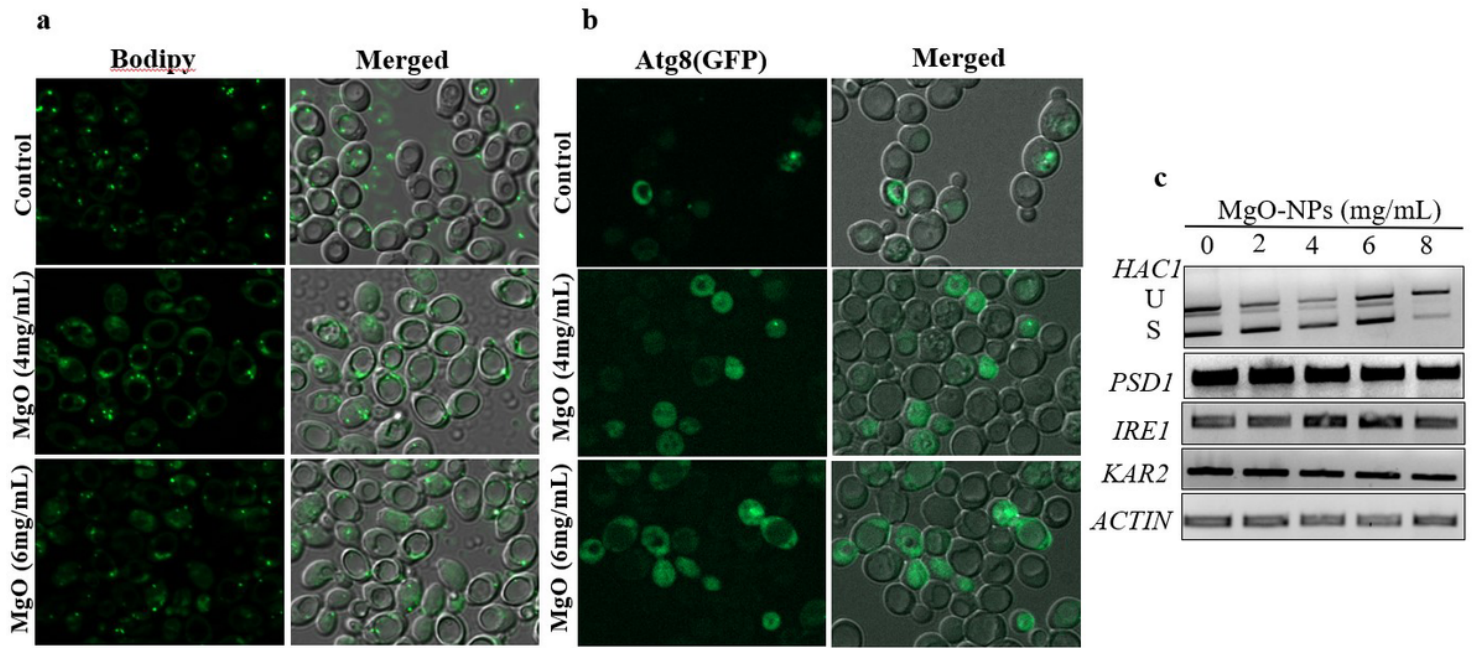
Figure 2

MgO-NPs toxicity cause upregulation in the chitin expression and its synthesis **(a)**Fluorescence microscopy image of CFW staining of yeast cells under controlled and 3h treated (4mg/ml) condition under DAPI filter **(b)**The gene expression analysis of *CHS* gene taking *ACTIN* as a reference **(c)** Band intensity of *CHS* genes measured by Image J. * indicates a significant difference between the untreated and treated groups (P<0.05).
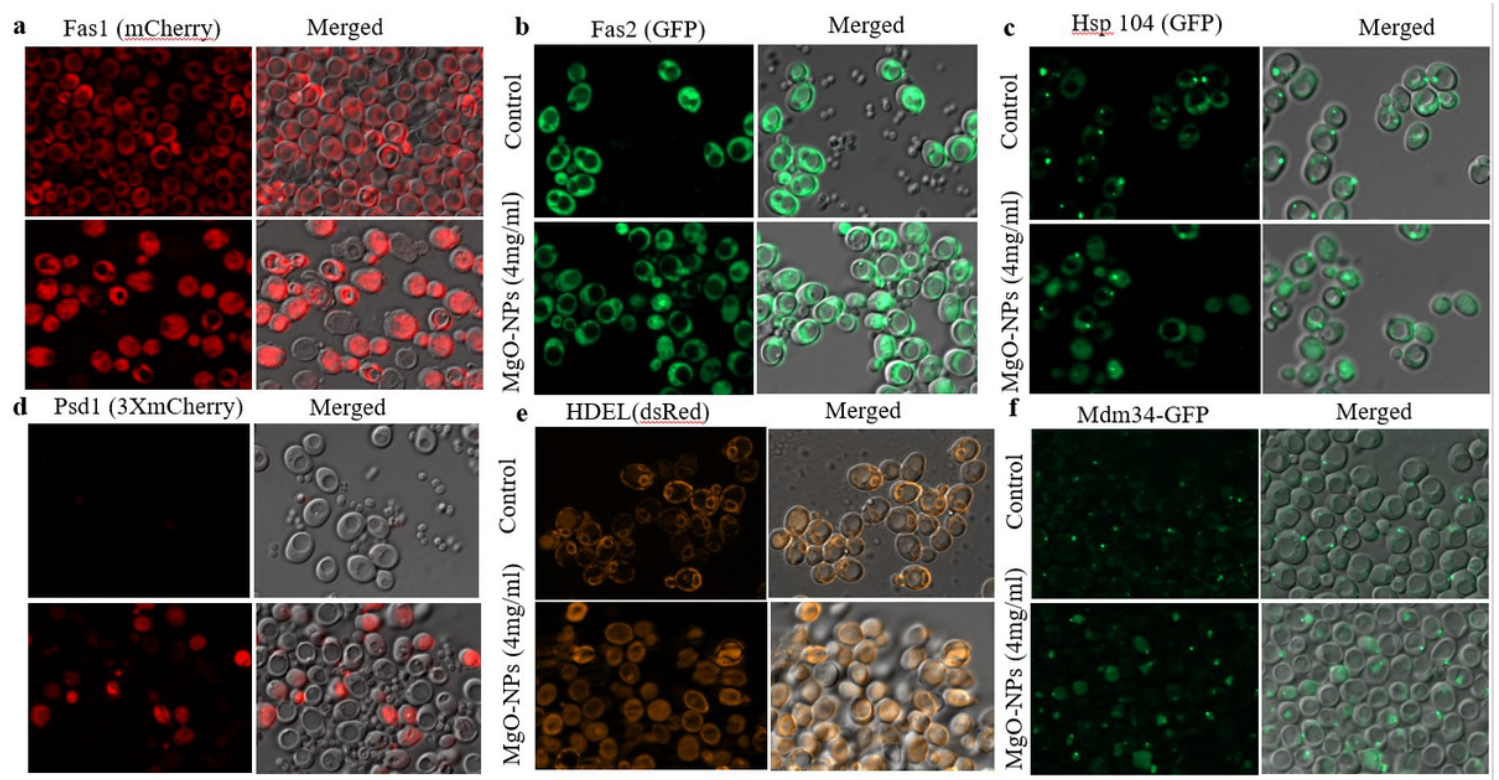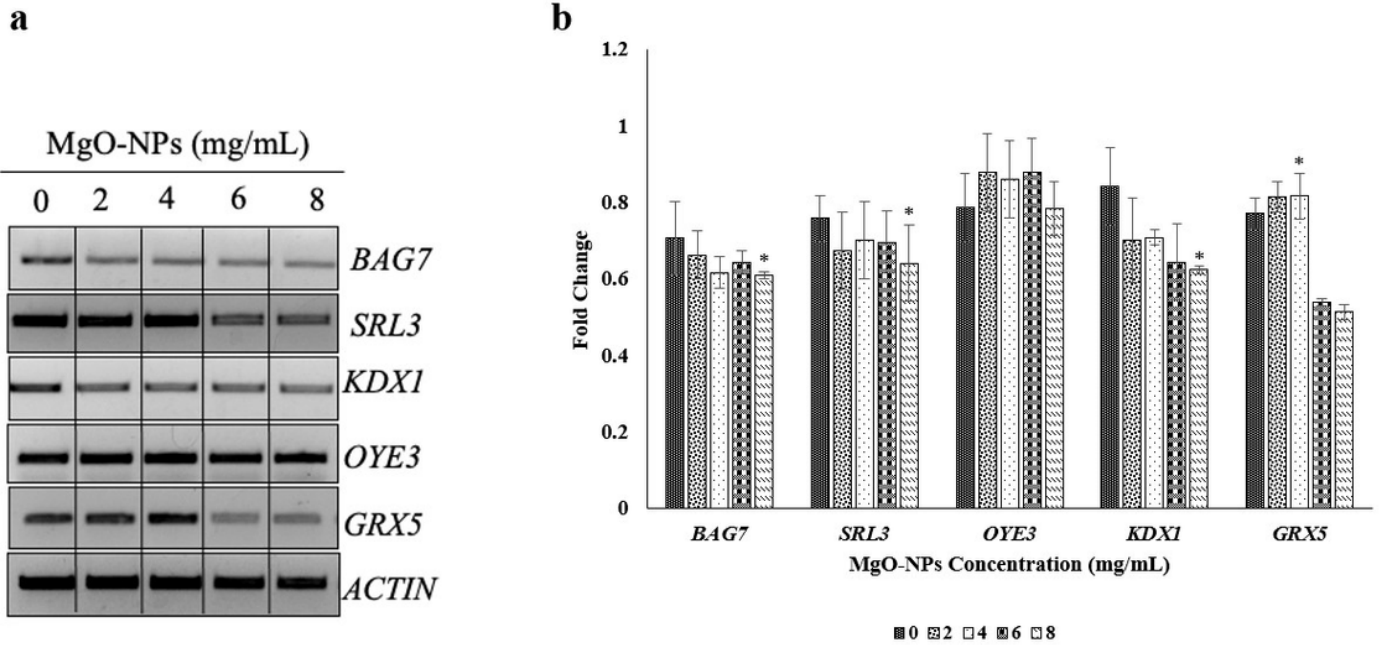

Figure 3

MgO-NPs have been found to impact lipid homeostasis, endoplasmic reticulum structure, and mitochondrial architecture, and trigger a heat shock response. These nanoparticles also affect the enzymes responsible for lipid biosynthesis. Fluorescence microscopy data **(a)** Fas1 and **(b)**Fas2 revealed that cells exposed to MgO-NPs displayed distinctive puncta or foci, whereas control cells exhibited homogeneous fluorescence. **(c)** The cells treated with MgO-NPs displayed prominent foci of Hsp-104, indicative of a heat shock response, while untreated cells had homogeneous distribution. **(d)** Furthermore, exposure to MgO-NPs resulted in alterations in the organization of mitochondria, as control cells exhibited mitochondrial localization of Psd1-3Xmcherry foci, whereas MgO-NPs exposed cells displayed altered localization throughout the cells. **(e)** MgO-NPs exposure caused changes in the distribution of ss-dsRed-HDEL, indicating perturbation in the endoplasmic reticulum architecture. **(f)** Exposure to MgO-NPs led to the loss of the ERMES complex, as control cells displayed distinct puncta of Mdm34-GFP with intense fluorescence, whereas treated cells had homogeneous distribution.
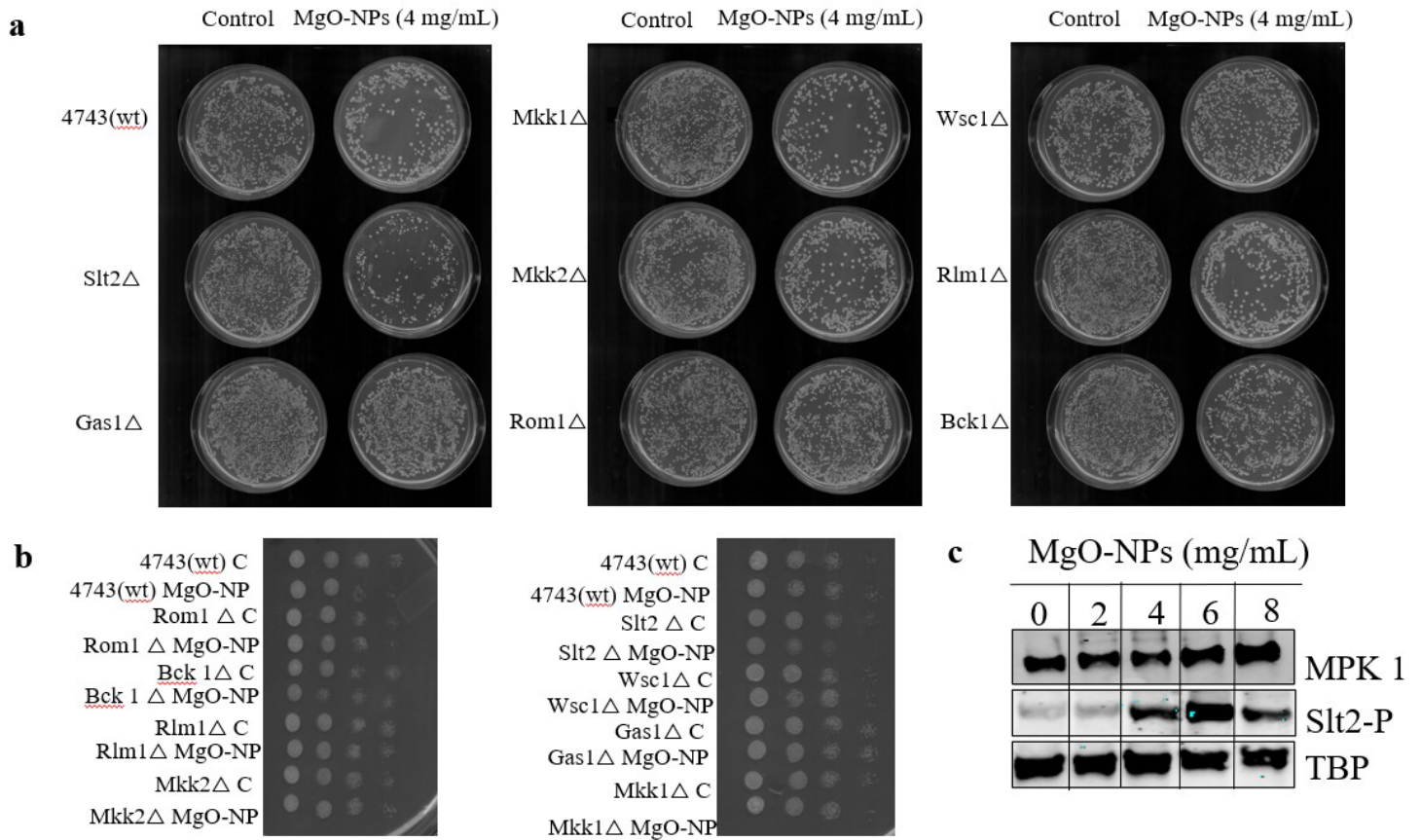
Figure 4

MgO-NPs induce the formation of lipid droplets, induce autophagy and activates Unfolded Protein Response (UPR). **(a)** After Bodipy staining, treated cells showed a higher number of lipid droplets (LDs) with green fluorescence compared to untreated (control) cells, indicating that MgO -NPs induce the formation of LDs. **(b)** MgO-NPs treatment caused the formation of intense foci of Atg8-GFP in cells, indicating the activation of autophagy, while control cells showed a homogenous distribution of Atg8-GFP. **(c)** MgO -NPs treatment leads to accumulation of active HAC1 precursor mRNA thus indicates the ER stress; *HAC1* splicing was tested by PCR (U-unspliced; S-spliced form of *HAC1*)

Note: To make the labelling within the figure, the MgO-NPs has been written as MgO.

Figure 5

The expression levels of specific stress-responsive genes (a) The expression has been analyzed using semi qPCR, *ACTIN* was used as a reference gene for loading control. (b)The intensity of the bands obtained from the PCR products was measured using ImageJ software. The results were plotted, and error bars were added to indicate the standard deviation of the measurements. * indicates a significant difference between the untreated and treated groups (P<0.05).

Figure 6

The elimination of CWI pathway proteins is crucial for cell survival under MgO-NPs imposed toxicity. **(a)** Wild type (BY4743) and null mutant strains of CWI pathway were subjected to untreated and treated conditions with MgO-NPs (4mg/ml) and 10-fold serially diluted cells were spread on YPD agar plates. **(b)** Similarly, the diluted cells were spotted on YPD agar plate and images were taken through scanner after 48h incubation at 30°C. **(c)** Immunoblot results showing activation of Slt2 kinase of CWI pathway where Anti-Tbp has taken as a loading control.
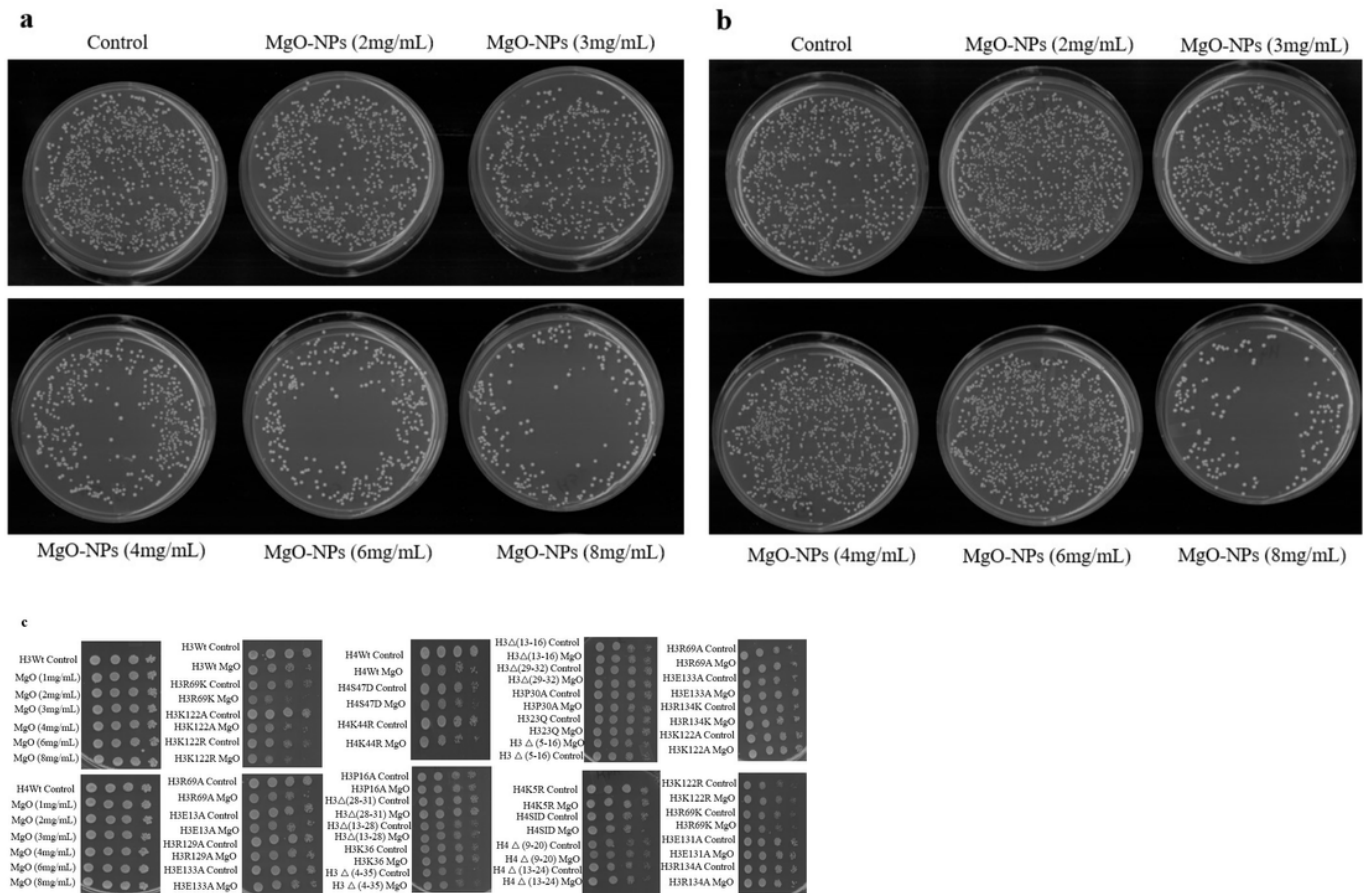
Figure 7

Growth inhibition analysis of histone H3 and H4 in the presence of MgO-NPs. **(a,b)** The exponentially growing wild type of histone H3 **(a)** and H4 **(b)** yeast cells were subjected to treated and untreated conditions with MgO-NPs in the range of 2mg/ml - 8mg/ml. cells were plated on YPD after 10 fold serial dilution. **(c)** Both histone H3 and H4 wild type along with mutants were treated with 4mg/ml MgO-NP and spotted on YPD plates after 10-fold serial dilution incubated at 30° C and then scanned after 48h.

Note: To make the labelling of all the strains in figure 7c the MgO-NPs has been written as MgO.

Supplementary Files

This is a list of supplementary files associated with this preprint. Click to download.

- SupplementaryInformation.docx